Supporting information (SI) for

Effects of perfluoroalkyl and polyfluoroalkyl substances (PFAS) on soil structure and function

*Baile Xu[1,2] *, Gaowen Yang[1,2], Anika Lehmann[1,2], Sebastian Riedel[3], Matthias C. Rillig[1,2]*

[1]Freie Universität Berlin, Institute of Biology, D-14195 Berlin, Germany

[2]Berlin-Brandenburg Institute of Advanced Biodiversity Research, D-14195 Berlin, Germany

[3]Freie Universität Berlin, Institute of Chemistry and Biochemistry, D-14195 Berlin, Germany

**Corresponding author. E-mail: bxu@zedat.fu-berlin.de*

Text S1 Details on the determination of PFAS concentrations in soil

After harvest, the air-dried soil samples were stored at –20 °C before analysis. The chemical analysis was performed at Bundesanstalt für Materialforschung und -prüfung (BAM), Berlin, Germany. The PFAS concentration was not directly measured, but converted based on the extracted organically bound fluorine in soil. The detailed procedures are described in a previous study (Metzger et al. 2019). The determined concentrations of PFAS are listed in Table S2.

We also found that the blank control contained tens of ng g^{-1} of organic fluorine (Table S2). This could be the case, because we determined fluorinated organic substances in soil, but not our target PFAS, so these fluorinated organic substances can be derived from other fluorine-containing organic agrochemicals. Meanwhile, due to the relatively high content of fluorinated organic substances in the blank soil, the determination of low concentrations of PFAS (i.e., < 100 ng g^{-1}) was inevitably accompanied with large errors. Even so, an apparent gradient of PFAS concentration was successfully achieved, which reached our objectives to understand soil response to gradients of PFAS concentrations.

Text S2 Details on the measurements of the proxies of soil health and function

Litter decomposition

Litter bags were produced to investigate the effects of PFASs on microbial decomposition of organic matters, which is the most common approach to measure litter decomposition rate (Kurz-Besson et al. 2005; Xie 2020). A nylon mesh (30 μm) was manually cut, folded and filled with pre-weighed 300 mg commercial green tea (Sichuan Mingshan Tea Co., China). We used an impulse sealer (Mercier Corp.) to seal the litter bag up, with a size of 2.5 ×1.5 cm (Lehmann et al. 2020). Sealed bags were microwaved for 30 sec to minimize their microbial communities and buried in the middle depth of 30 g soil when placed into each tube. At the end of incubation, litter bags were picked up, rinsed by deionized water to remove adhered soil particles and dried at 60 °C. The reduced mass of green tea was employed as an indication of decomposition (%).

Soil respiration

Soil respiration was determined twice, after the 3- and 6-week incubation. We opened the cap of each tube for 5 mins to equilibrate the air in the tube with the ambient environment, and changed to the airtight cap with rubber stoppers. Meanwhile, 1 ml of air was sampled for the headspace of each tube as the initial point. After 4 h incubation, another 1 ml of air was sampled as the final point. Concentrations of CO_2 in sampled air were determined by an infrared gas analyzer (LI-6400XT, LiCOR GmbH), and soil respiration was reported as the net CO_2 production (μM M^{-1}).

Soil pH

A portion of 2 g air-dried soil samples was mixed with 10-mL deionized water, and shaken horizontally at 250 rpm for 30 min at room temperature (20°C). Soil solution was centrifuged at 3000 rpm for 5 min and pH was measured in the supernatant with a pH meter (Hanna Instruments, Smithfield, USA).

Soil enzyme and microbial activities

After incubation, a portion of 5 g fresh soil was collected to measure four functional enzymes related to C, N and P cycling, i.e., β-glucosidase and β-D-1,4-cellobiosidase (C-related), β-1,4-N-acetyl-glucosaminidase (N-related), and phosphatase (P-related). In addition, a portion of 1 g fresh soil was sampled to measure the fluorescein diacetate hydrolase (FDA) activity as an indicator of general microbial activity. Fresh soil samples were stored at 4°C before analysis, and all enzyme activities were determined in two weeks using high-throughput microplate assays (Benchmark Microplate reader, Bio-Rad Lab., Inc.). Detailed protocols were described in previous studies (Jackson et al. 2013; Liang et al. 2019).

Water-stable soil aggregates

Water-stable aggregates (WSA) were quantified by the method of (Kemper and Rosenau 1986), as described in (Liang et al. 2019). In brief, 4 g dried soil was placed on a 250-μm sieve, rewetted using the capillary method, and then immersed in a wet-sieving apparatus (Eijkelkamp, Netherlands) with deionized water for 5 min. The remaining fraction on the sieve was collected and dried at 60 °C. The percentage of

WSA (%) was calculated after coarse matters deducted, following WSA (%) = (remaining fraction – coarse matter) / (4.0 – coarse matter).

Soil DNA extraction and qPCR

We weighed approximately 250 mg fresh soil previously stored at −80 °C to extract soil DNA using DNeasy PowerSoil Pro Kit (QIAGEN GmbH, Germany), following the technical protocol. A portion DNA solution was diluted five times and stored at −20 °C for further analysis.

Quantitative polymerase chain reactions (qPCR) was operated in a CFX 96 Real-Time System (Touch 1009, Bio-Rad Lab., Inc, USA) in 96-well plates. Soil DNA was amplified with the universal primer 515F (5'-GTGCCAGCMGCCGCGGTAA-3') and 806R (5'-GGACTACHVGGGTWTCTAAT-3') for soil bacteria with the KAPA HiFi PCR kit (Roche GmbH, Germany). Each reaction of a volume of 20 µL contained 1×KAPA HiFi buffer, 0.3 mM KAPA dNTP Mix, 0.75 µM of each primer, 0.1 U KAPA HiFi Polymerase, 0.5 µM EvaGreen Fluorescent DNA Stain (Jena Bioscience GmbH, Germany), and 5 µL DNA template. The thermocycler conditions for bacterial qPCR were: 3 min of initial denaturation at 95 °C, followed by 30 cycles of 20 s of denaturation at 95 °C, 30 s of annealing at 50 °C, and 30 s of extension at 68 °C, and ended with 5 min of final extension at 68 °C; for fungal qPCR: 3 min of initial denaturation at 95 °C, followed by 30 cycles of 15 s of denaturation at 98 °C, 45 s of annealing and extension at 67 °C, and ended with 5 min of final extension at 72 °C. The melting curves was tested from 65 °C to 95 °C to check the specific amplification product. All analyses were performed in triplicates, and negative controls with were also conducted in each plate. Standards for calibration were prepared from PCR amplified genes from DNA pool. The amplification product was confirmed in agarose gel for the specificity and size. After the purification with magnetic beads, the DNA concentration of PCR products was measured using a Qubit 3 Fluorometer (Fisher Scientific GmbH, Germany), and diluted to an appropriate series of points for qPCR standards. Standard curves had R^2 values higher than 0.997, and amplification efficiencies were 89% ± 1%, and 93% ± 3% for bacterial and fungal primers, respectively.

Table S1 Basic properties of selected PFASs.

PFAS	Purity	manufacturer	Chemical structure	Molecular formula	Molecular weight (g mol^{-1})	Water solubility	pK_a [a]	Log K_{ow} [b]
Perfluorooctane sulfonic acid (PFOS)	98%	TCI Co., Ltd.	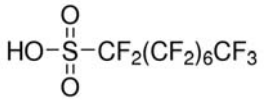	$C_8HF_{17}SO_3$	500.1	Soluble [c]	<1.0	5.26
Perfluorooctanoic acid (PFOA)	98%	Strem Chemicals Inc.	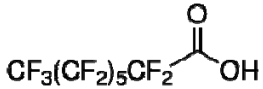	$C_8HF_{15}O_2$	414.0	3.4 g L^{-1} (20°C) [c]	-0.5–4.2	4.59
Perfluorobutanesulfonic acid (PFBS)	97%	Sigma-Aldrich Corp.	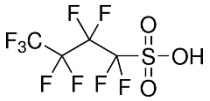	$C_4HF_9SO_3$	300.1	344 mg L^{-1} (25°C) [a]	-3.31	2.73

[a] Acid dissociation constant, data from PubChem (https://pubchem.ncbi.nlm.nih.gov)
[b] Octanol-water partition coefficient, data from ref. (Milinovic et al. 2015)
[c] Data sheet from manufacturer

Table S2 The actual concentrations of PFAS in each treatment and blank control. Note that the blank control contained tens of ng g^{-1} of organic fluorine, and it was deducted for calculating the actual concentration of each PFAS.

PFOS (ng g^{-1})		PFOA (ng g^{-1})		PFBS (ng g^{-1})	
Nominal concentration	Actual concentration	Nominal concentration	Actual concentration	Nominal concentration	Actual concentration
1	9.23 ± 10.09	1	4.14 ± 9.83	0.5	3.51 ± 1.71
10	11.48 ± 6.89	10	15.23 ± 4.37	5	6.90 ± 0.10
100	118.48 ± 18.19	100	110.58 ± 16.81	50	59.69 ± 0.72
1000	1180.57 ± 48.17	1000	1224.68 ± 142.48	500	580.10 ± 17.54
Blank control	54.45 ± 8.94	Blank control	118.15 ± 21.42	Blank control	34.86 ± 2.00

Table S3 Outcomes of multiple comparison of treatments with the control for soil functions. The p-value < 0.05 was considered significant and marked in bold. In the PFAS treatment, the first column represents each concentration of four PFASs.

Treatment − control ≥ 0	Decomposition		Soil respiration week 3		Soil respiration week 6		Water-stable aggregates		Bacterial abundance		Fungal abundance	
	t-value	p-value	t-value	p-value	t-value	p-value	t-value	p-value	t-value	p-value	t-value	p-value
PFAS treatment												
PFOS_1	1.250	0.854	-0.954	0.971	0.720	0.997	-1.551	0.643	2.038	0.3065	-0.037	1
PFOS_10	-0.828	0.990	0.484	1.000	1.057	0.943	-1.163	0.900	0.073	1	-0.669	0.998
PFOS_100	0.850	0.988	-2.470	0.126	0.887	0.983	-2.462	0.129	1.636	0.5785	-0.557	1
PFOS_1000	2.679	0.077	-2.154	0.246	0.263	1.000	-2.160	0.243	1.112	0.9223	0.018	1
PFOA_1	1.294	0.827	-2.603	0.092	-0.039	1.000	-1.240	0.859	2.671	0.0784	-0.553	1
PFOA_10	1.589	0.615	-4.700	**< 0.001**	-1.587	0.616	-1.263	0.846	0.752	0.9955	-0.203	1
PFOA_100	2.638	0.085	-4.276	**< 0.001**	-0.389	1.000	-2.650	0.083	0.462	1	-0.459	1
PFOA_1000	4.283	**< 0.001**	-2.046	0.302	1.494	0.687	-1.057	0.943	0.806	0.9919	-0.316	1
PFBS_0.5	3.998	**0.001**	-4.026	**0.001**	-1.643	0.573	-0.100	1.000	0.059	1	-2.125	0.26
PFBS_5	5.189	**< 0.001**	-4.394	**< 0.001**	-0.066	1.000	0.297	1.000	2.72	0.0694	-1.323	0.809
PFBS_50	3.991	**0.001**	-3.158	**0.021**	-1.633	0.581	-0.041	1.000	2.324	0.174	-2.08	0.284
PFBS_500	2.858	**0.049**	-4.987	**< 0.001**	-3.193	**0.019**	-2.242	0.207	1.964	0.35	-0.572	1
PFAS type												
PFOS	1.197	0.410	-1.572	0.225	0.918	0.593	-2.366	**0.044**	1.532	0.2415	-0.419	0.922
PFOA	2.971	**0.008**	-4.205	**<0.001**	-0.164	0.994	-2.003	0.098	1.479	0.2644	-0.515	0.871
PFBS	4.860	**<0.001**	-5.112	**<0.001**	-2.049	0.089	-0.673	0.768	2.228	0.0599	-2.05	0.089

Table S3 Continued

Treatment − control ≥ 0	β-glucosidase		β-D-cellobiosidase		β-N-glucosaminidase		Phosphatase		FDA		pH	
	t-value	p-value	t-value	p-value	t-value	p-value	t-value	p-value	t-value	p-value	t-value	p-value
PFAS treatment												
PFOS_1	0.333	1.000	-1.086	0.932	0.690	0.998	-0.195	1.000	0.072	1.000	1.481	0.68503
PFOS_10	0.946	0.973	0.351	1.000	1.792	0.463	1.101	0.927	-0.700	0.998	0.984	0.96067
PFOS_100	1.545	0.648	0.271	1.000	2.244	0.206	0.874	0.985	-0.148	1.000	-0.01	1
PFOS_1000	1.387	0.765	-0.892	0.982	0.942	0.974	0.425	1.000	-0.080	1.000	2.038	0.29987
PFOA_1	1.476	0.701	0.153	1.000	0.988	0.963	0.817	0.991	1.003	0.959	2.821	0.05273
PFOA_10	1.907	0.386	0.177	1.000	2.636	0.086	0.398	1.000	2.197	0.226	2.535	0.10665
PFOA_100	0.256	1.000	0.714	0.997	1.042	0.948	-0.475	1.000	0.388	1.000	1.421	0.72909
PFOA_1000	0.818	0.991	-0.675	0.998	1.187	0.888	-0.273	1.000	1.563	0.634	4.076	**0.00111**
PFBS_0.5	2.147	0.250	-0.633	0.999	0.637	0.999	0.295	1.000	0.363	1.000	3.092	**0.02532**
PFBS_5	1.858	0.417	0.347	1.000	0.166	1.000	0.220	1.000	1.169	0.897	3.528	**0.00691**
PFBS_50	1.733	0.506	0.588	1.000	1.744	0.498	1.551	0.644	0.789	0.993	3.769	**0.00305**
PFBS_500	1.827	0.439	-0.413	1.000	1.309	0.817	1.197	0.883	1.483	0.695	4.251	**< 0.001**
PFAS type												
PFOS	1.409	0.297	-0.449	0.908	1.857	0.132	0.732	0.726	-0.286	0.972	1.425	0.28492
PFOA	1.491	0.259	0.122	0.998	1.917	0.117	0.155	0.995	1.719	0.173	3.474	**0.00218**
PFBS	2.532	**0.029**	-0.036	1.000	1.263	0.372	1.084	0.480	1.269	0.369	4.644	**< 0.001**

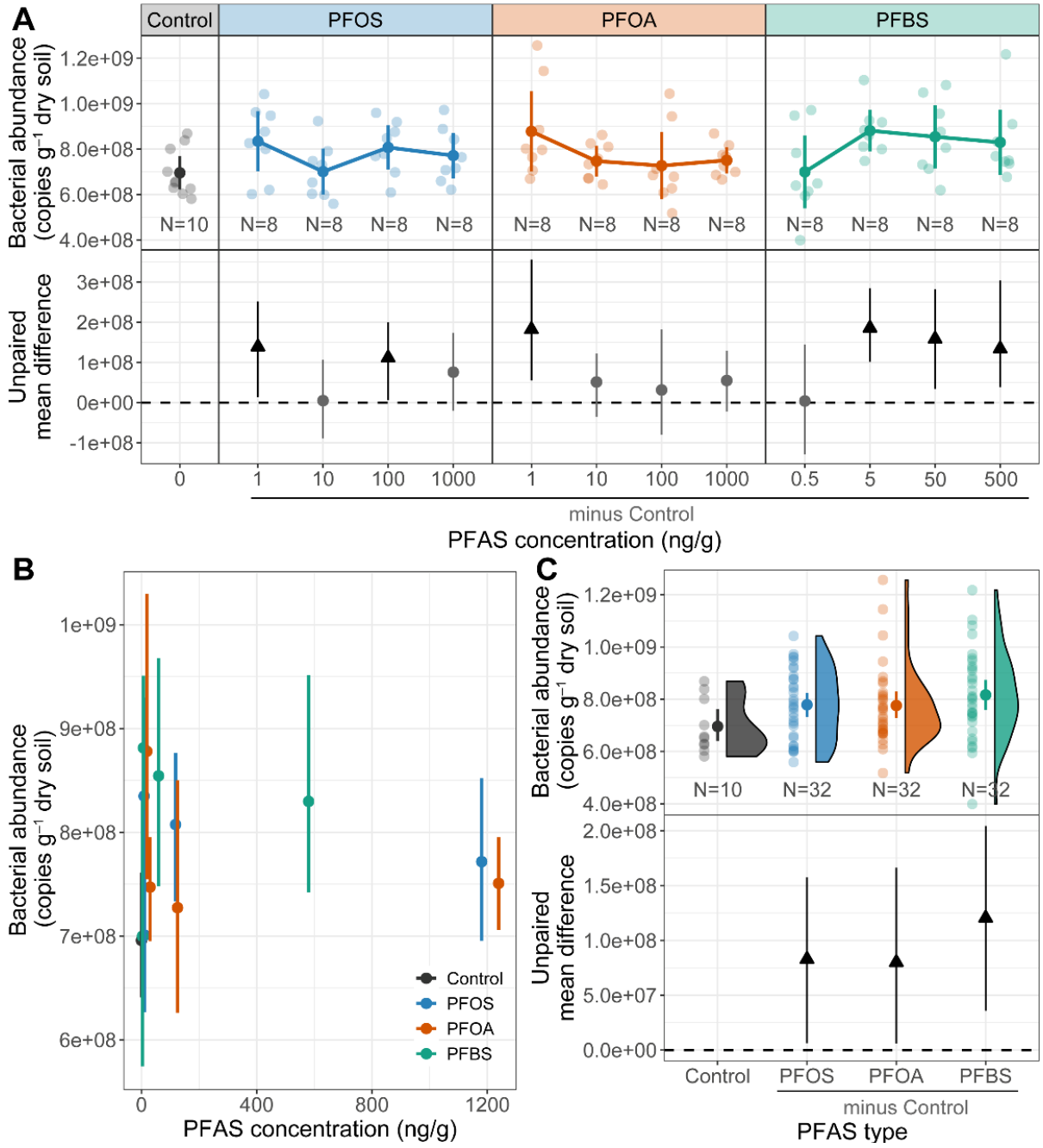

Figure S1. Effects of per- and polyfluoroalkyl substances (PFASs) on soil bacterial abundance. (A) Visualization of the effect of each PFAS on soil bacterial abundance over the range of treatment concentrations (first row). Raw data are presented as both scatter points and the corresponding mean and 95% confidence intervals (CIs) (N = 8 for each treatment, and N = 10 for blank control). (B) Summary of effects of actual PFAS concentrations on soil bacterial abundance combining treatment types. (C) Summary of PFAS type effects on soil bacterial abundance combining treatment concentrations. Data in the first row of (C) are presented in raincloud plots supplemented with the corresponding mean and 95% CIs. In the second row, estimation plots present the unpaired mean difference between each treatment

and the shared control. Circles in grey represent neutral effects (95% CIs overlapping the dashed zone line), and triangles (arrow head up) in black represent positive effects (no overlapping of 95% CIs with the dashed zero line). PFOS, perfluorooctanesulfonic acid; PFOA, perfluorooctanoic acid; PFBS, perfluorobutanesulfonic acid. The outcome of ANOVA followed by Dunnett's test is presented in Table S3.

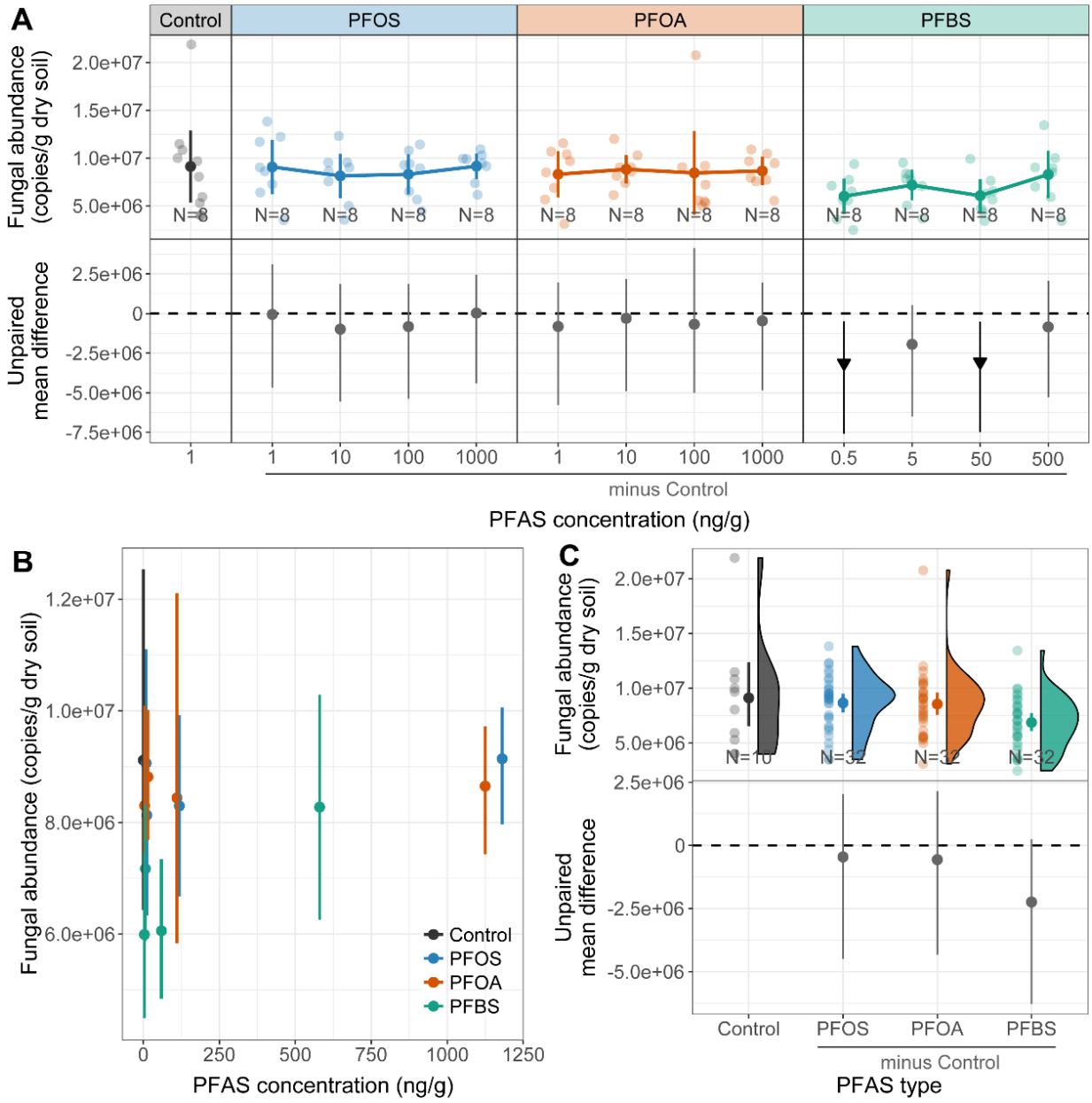

Figure S2. Effects of per- and polyfluoroalkyl substances (PFASs) on soil fungal abundance. (A) Visualization of the effect of each PFAS on soil fungal abundance over the range of treatment concentrations (first row). Raw data are presented as both scatter points and the corresponding mean and 95% confidence intervals (CIs) (N = 8 for each treatment, and N = 10 for blank control). (B) Summary of effects of actual PFAS concentrations on soil fungal abundance combining treatment types. (C) Summary of PFAS type effects on soil fungal abundance combining treatment concentrations. Data in the first row of (C) are presented in raincloud plots supplemented with the corresponding mean and 95% CIs. In the second row, estimation plots present the unpaired mean difference between each treatment and the shared control. Circles in grey represent neutral effects (95% CIs overlapping the dashed zone line), and triangles (arrow head down) in black represent negative effects (no overlapping of 95% CIs with the

dashed zero line). PFOS, perfluorooctanesulfonic acid; PFOA, perfluorooctanoic acid; PFBS, perfluorobutanesulfonic acid. The outcome of ANOVA followed by Dunnett's test is presented in Table S3.

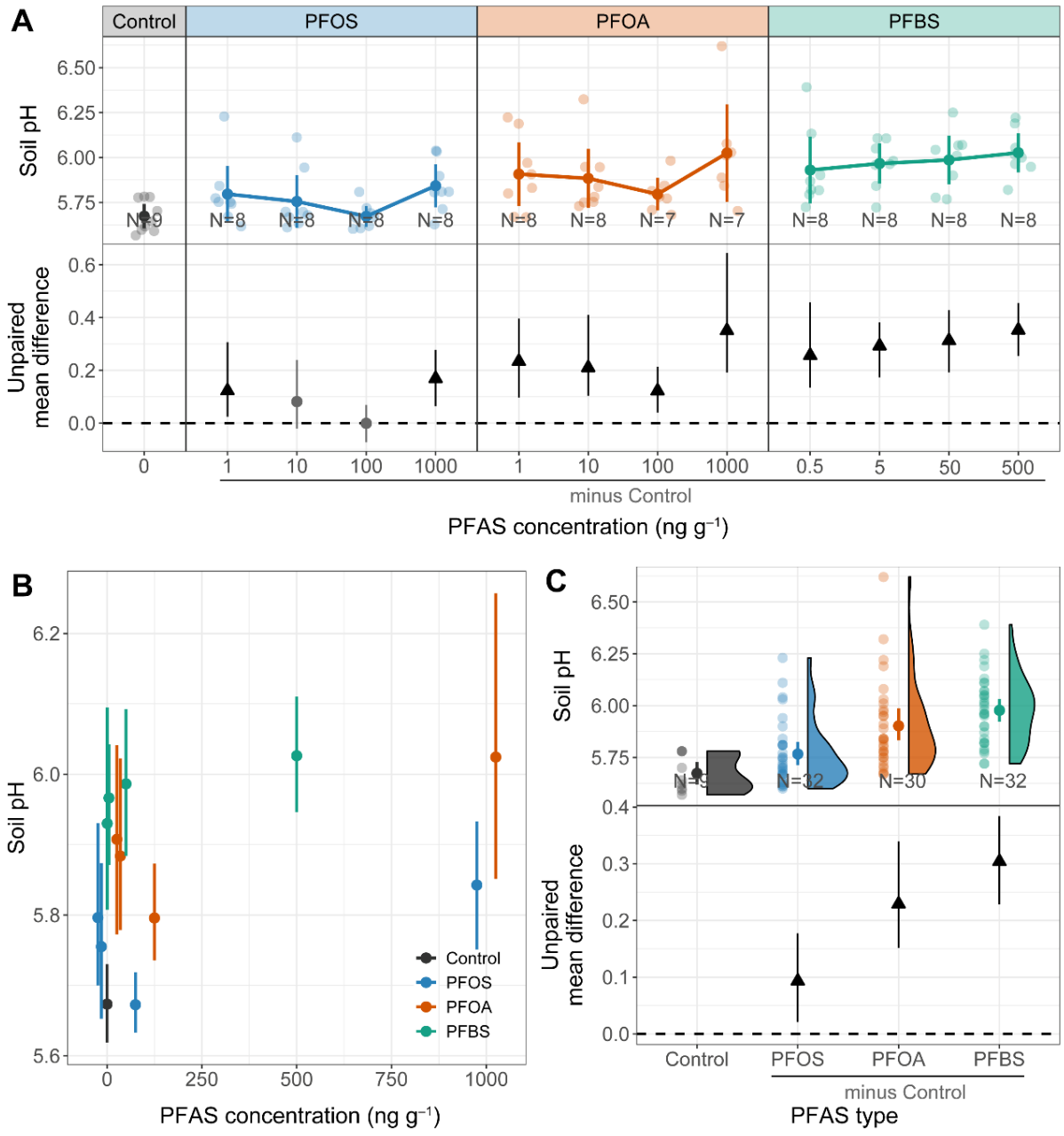

Figure S3. Effects of per- and polyfluoroalkyl substances (PFASs) on soil pH. (A) Visualization of the effect of each PFAS on soil pH over the range of treatment concentrations (first row). Raw data are presented as both scatter points and the corresponding mean and 95% confidence intervals (CIs) (N = 8 for each treatment, and N = 10 for blank control). (B) Summary of effects of actual PFAS concentrations on soil **pH** combining treatment types. (C) Summary of PFAS type effects on soil **pH** combining treatment concentrations. Data in the first row of (C) are presented in raincloud plots supplemented with the corresponding mean and 95% CIs. In the second row, estimation plots present the unpaired mean

difference between each treatment and the shared control. Circles in grey represent neutral effects (95% CIs overlapping the dashed zone line), and triangles (arrow head up) in black represent positive effects (no overlapping of 95% CIs with the dashed zero line). PFOS, perfluorooctanesulfonic acid; PFOA, perfluorooctanoic acid; PFBS, perfluorobutanesulfonic acid. The outcome of ANOVA followed by Dunnett's test is presented in Table S3.

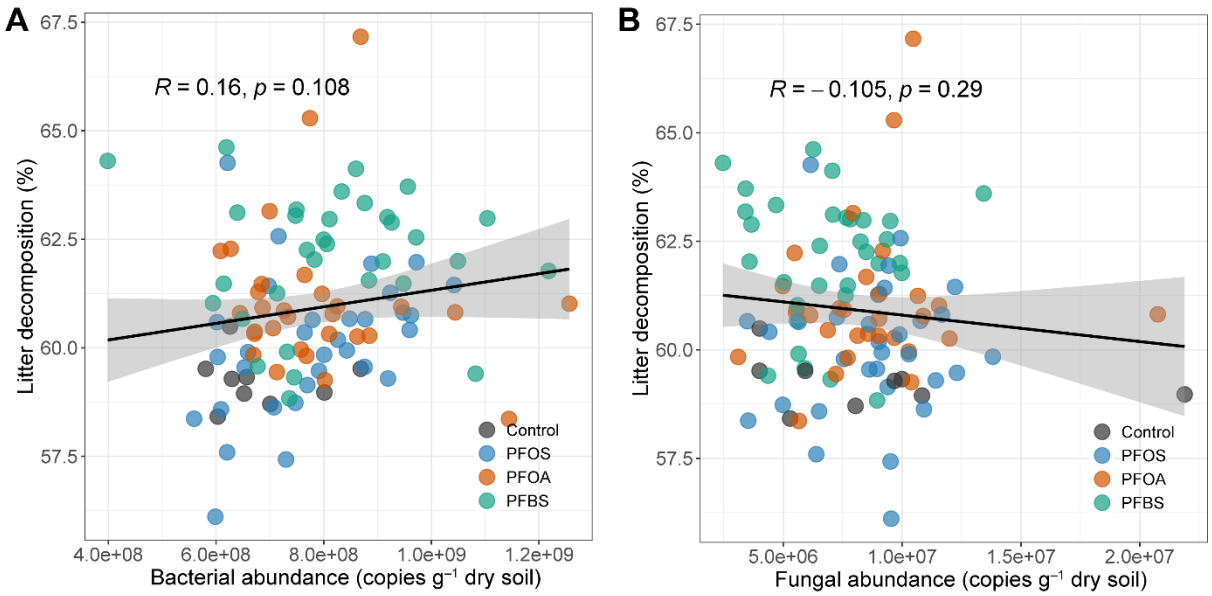

Figure S4. The correlations of litter decomposition with soil bacterial abundance (A) and fungal abundance (B), respectively.

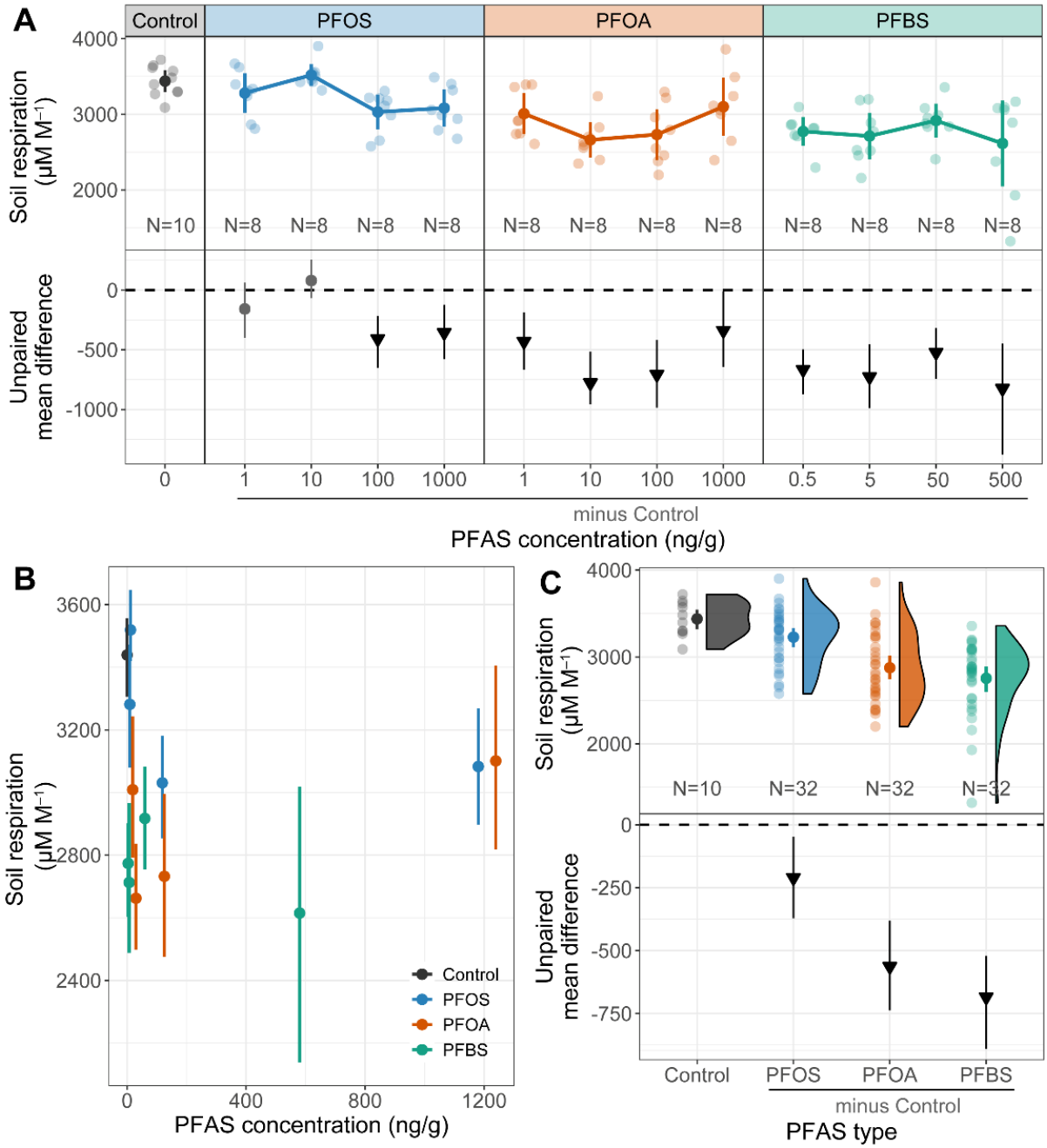

Figure S5. Effects of per- and polyfluoroalkyl substances (PFASs) on soil respiration in week 3. (A) Visualization of the effect of each PFAS on soil respiration over the range of treatment concentrations (first row). Raw data are presented as both scatter points and the corresponding mean and 95% confidence intervals (CIs) (N = 8 for each treatment, and N = 10 for blank control). (B) Summary of effects of actual PFAS concentrations on soil respiration combining treatment types. (C) Summary of PFAS type effects on soil respiration combining treatment concentrations. Data in the first row of (C) are presented in raincloud plots supplemented with the corresponding mean and 95% CIs. In the second row, estimation plots present the unpaired mean difference between each treatment and the shared control. Circles in

grey represent neutral effects (95% CIs overlapping the dashed zone line), and triangles (arrow head down) in black represent negative effects (no overlapping of 95% CIs with the dashed zero line). PFOS, perfluorooctanesulfonic acid; PFOA, perfluorooctanoic acid; PFBS, perfluorobutanesulfonic acid. The outcome of ANOVA followed by Dunnett's test is presented in Table S3.

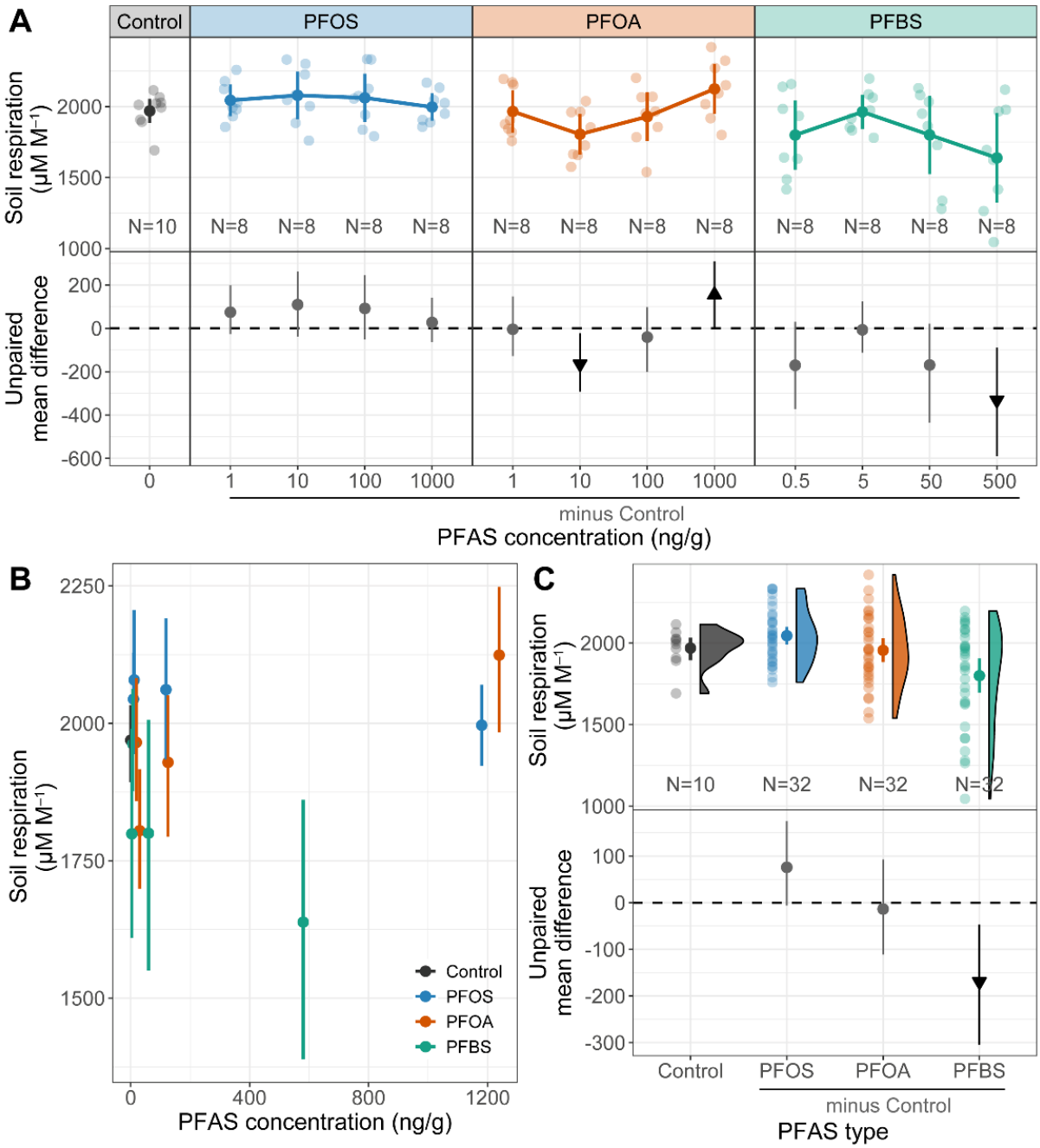

Figure S6. Effects of per- and polyfluoroalkyl substances (PFASs) on soil respiration in week 6. (A) Visualization of the effect of each PFAS on soil respiration over the range of treatment concentrations (first row). Raw data are presented as both scatter points and the corresponding mean and 95% confidence intervals (CIs) (N = 8 for each treatment, and N = 10 for blank control). (B) Summary of effects of actual PFAS concentrations on soil respiration combining treatment types. (C) Summary of PFAS type effects on soil respiration combining treatment concentrations (first row). Data in the first row of (C) are presented in raincloud plots supplemented with the corresponding mean and 95% CIs. In the second row, estimation plots present the unpaired mean difference between each treatment and the shared control.

Circles in grey represent neutral effects (95% CIs overlapping the dashed zone line), and triangles with arrow head up and down in black represent positive and negative effects respectively (no overlapping of 95% CIs with the dashed zero line). PFOS, perfluorooctanesulfonic acid; PFOA, perfluorooctanoic acid; PFBS, perfluorobutanesulfonic acid. The outcome of ANOVA followed by Dunnett's test is presented in Table S3.

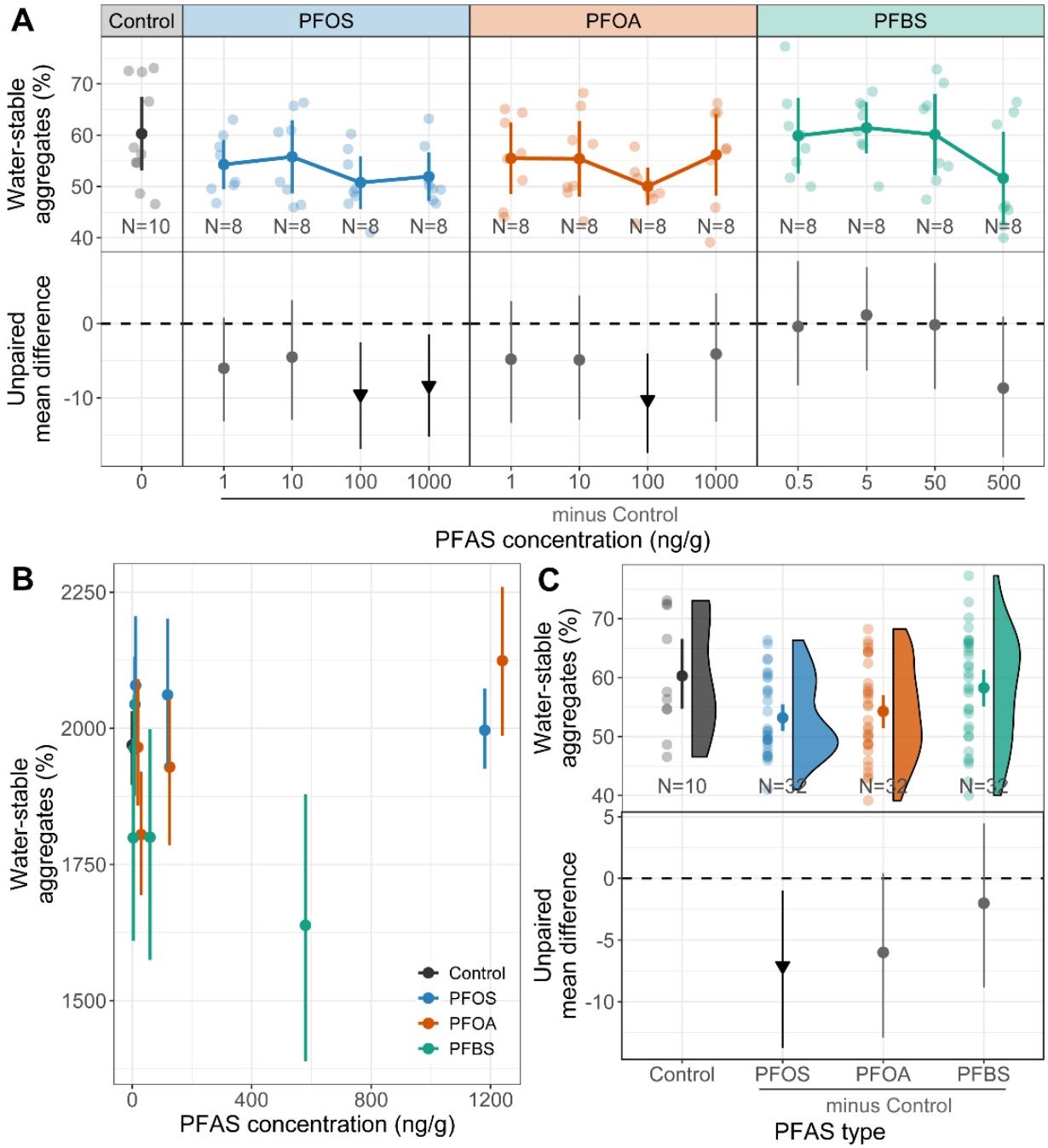

Figure S7. Effects of per- and polyfluoroalkyl substances (PFASs) on soil water-stable aggregates. (A) Visualization of the effect of each PFAS on soil water-stable aggregates over the range of treatment concentrations (first row). Raw data are presented as both scatter points and the corresponding mean and 95% confidence intervals (CIs) (N = 8 for each treatment, and N = 10 for blank control). (B) Summary of effects of actual PFAS concentrations on soil water-stable aggregates combining treatment types. (C) Summary of PFAS type effects on soil water-stable aggregates combining treatment concentrations (first row). Data in the first row of (C) are presented in raincloud plots supplemented with the corresponding mean and 95% CIs. In the second row, estimation plots present the unpaired mean difference between

each treatment and the shared control. Circles in grey represent neutral effects (95% CIs overlapping the dashed zone line), and triangles with arrow head up and down in black represent positive and negative effects respectively (no overlapping of 95% CIs with the dashed zero line). PFOS, perfluorooctanesulfonic acid; PFOA, perfluorooctanoic acid; PFBS, perfluorobutanesulfonic acid. The outcome of ANOVA followed by Dunnett's test is presented in Table S3.

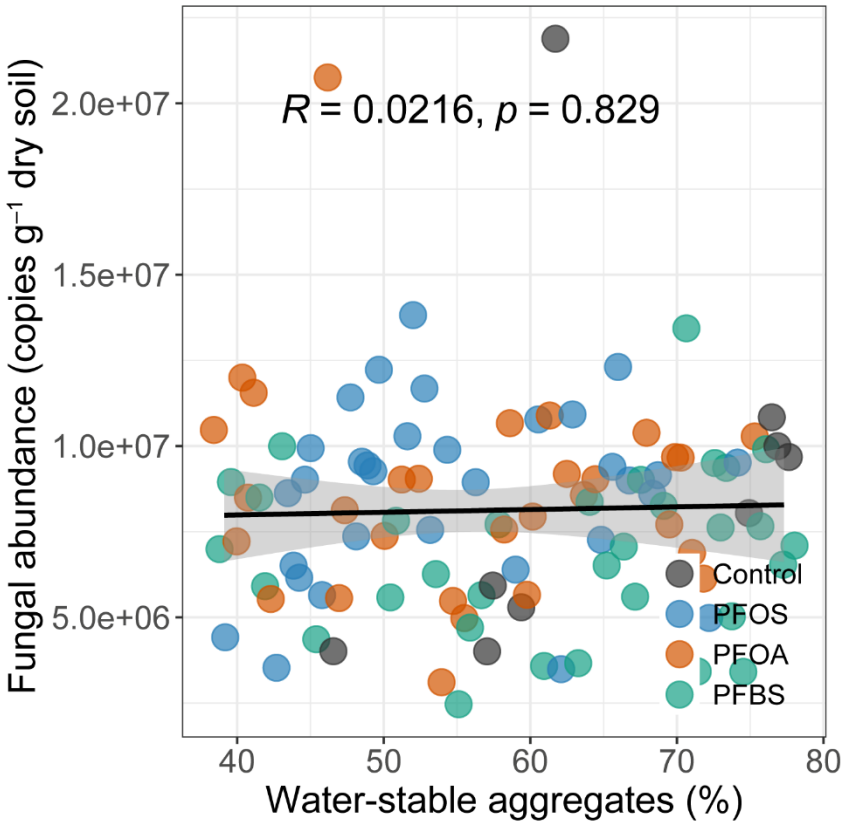

Figure S8. The correlation between soil water-stable aggregates and fungal abundance.

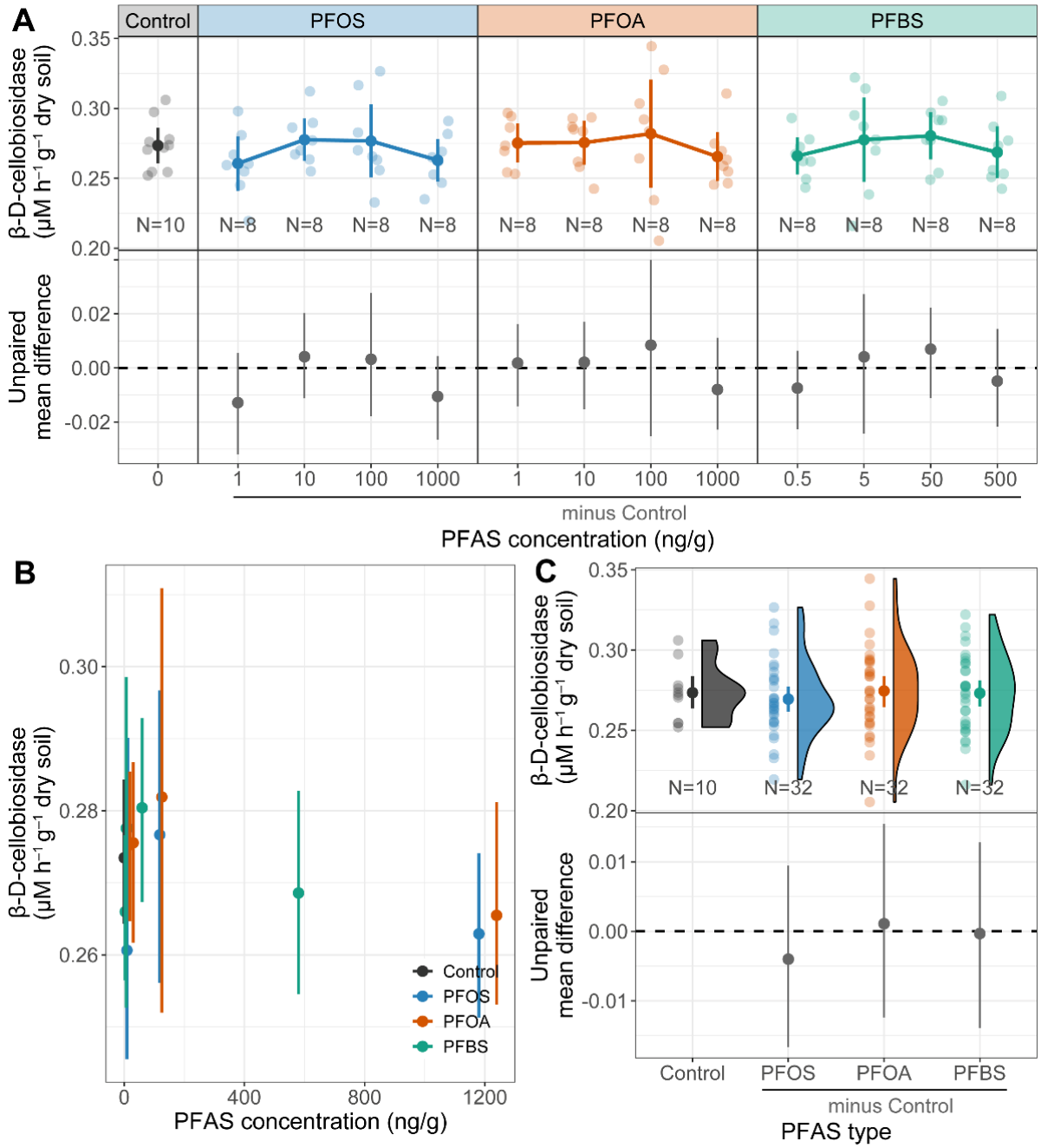

Figure S9. Effects of per- and polyfluoroalkyl substances (PFASs) on β-D-1,4-cellobiosidase activities. (A) Visualization of the effect of each PFAS on β-D-1,4-cellobiosidase activities over the range of treatment concentrations (first row). Raw data are presented as both scatter points and the corresponding mean and 95% confidence intervals (CIs) (N = 8 for each treatment, and N = 10 for blank control). (B) Summary of effects of actual PFAS concentrations on β-D-1,4-cellobiosidase activities combining treatment types. (C) Summary of PFAS type effects on β-D-1,4-cellobiosidase activities combining treatment concentrations (first row). Data in the first row of (C) are presented in raincloud plots supplemented with the corresponding mean and 95% CIs. In the second row, estimation plots present the unpaired mean

difference between each treatment and the shared control. Circles in grey represent neutral effects (95% CIs overlapping the dashed zone line). PFOS, perfluorooctanesulfonic acid; PFOA, perfluorooctanoic acid; PFBS, perfluorobutanesulfonic acid. The outcome of ANOVA followed by Dunnett's test is presented in Table S3.

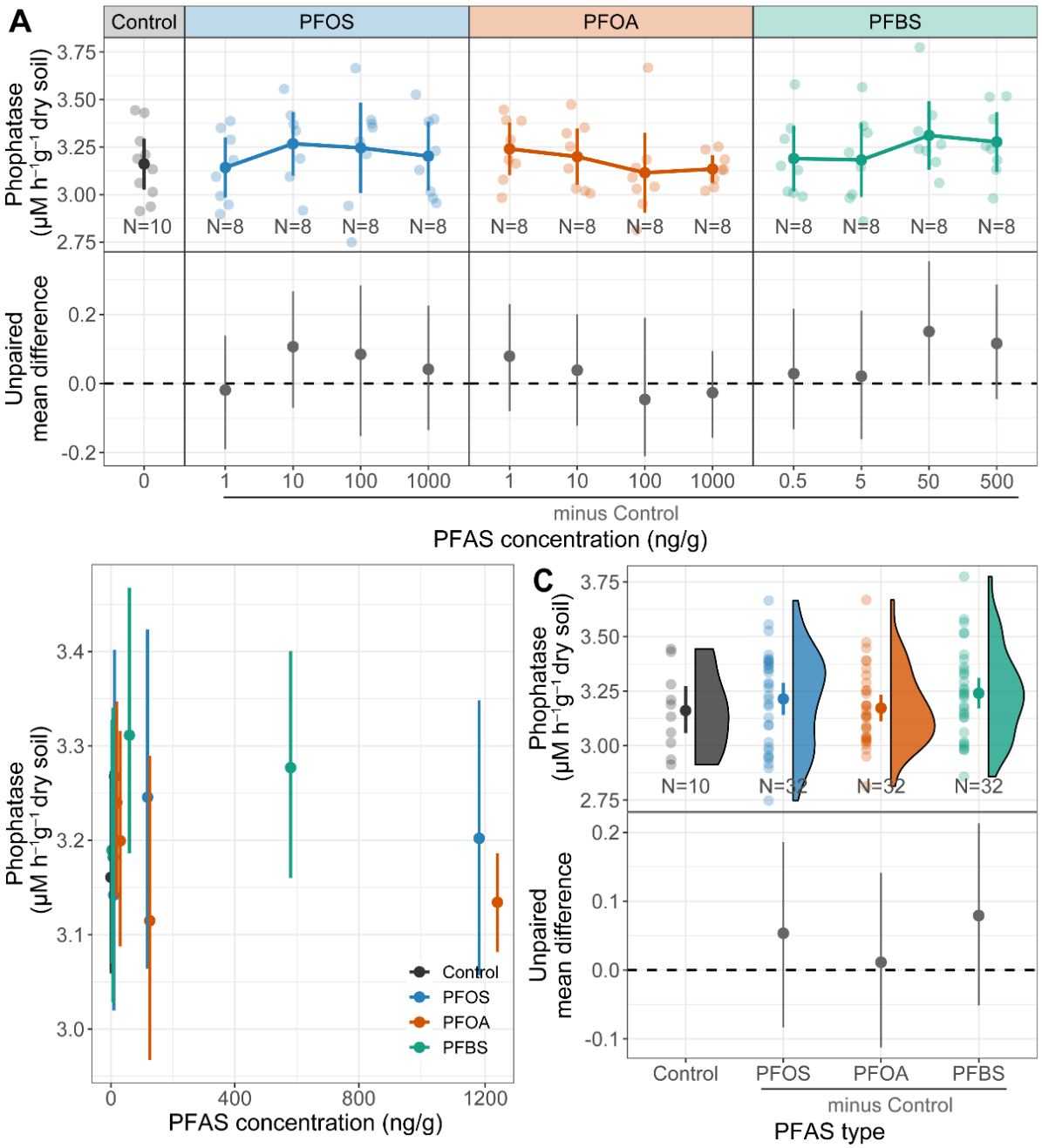

Figure S10. Effects of per- and polyfluoroalkyl substances (PFASs) on phosphatase activities. (A) Visualization of the effect of each PFAS on phosphatase activities over the range of treatment concentrations (first row). Raw data are presented as both scatter points and the corresponding mean and 95% confidence intervals (CIs) (N = 8 for each treatment, and N = 10 for blank control). (B) Summary of effects of actual PFAS concentrations on phosphatase activities combining treatment types. (C) Summary of PFAS type effects on phosphatase activities combining treatment concentrations (first row). Data in the first row of (C) are presented in raincloud plots supplemented with the corresponding mean and 95% CIs. In the second row of each panel, estimation plots present the unpaired mean difference

between each treatment and the shared control. Circles in grey represent neutral effects (95% CIs overlapping the dashed zone line). PFOS, perfluorooctanesulfonic acid; PFOA, perfluorooctanoic acid; PFBS, perfluorobutanesulfonic acid. The outcome of ANOVA followed by Dunnett's test is presented in Table S3.

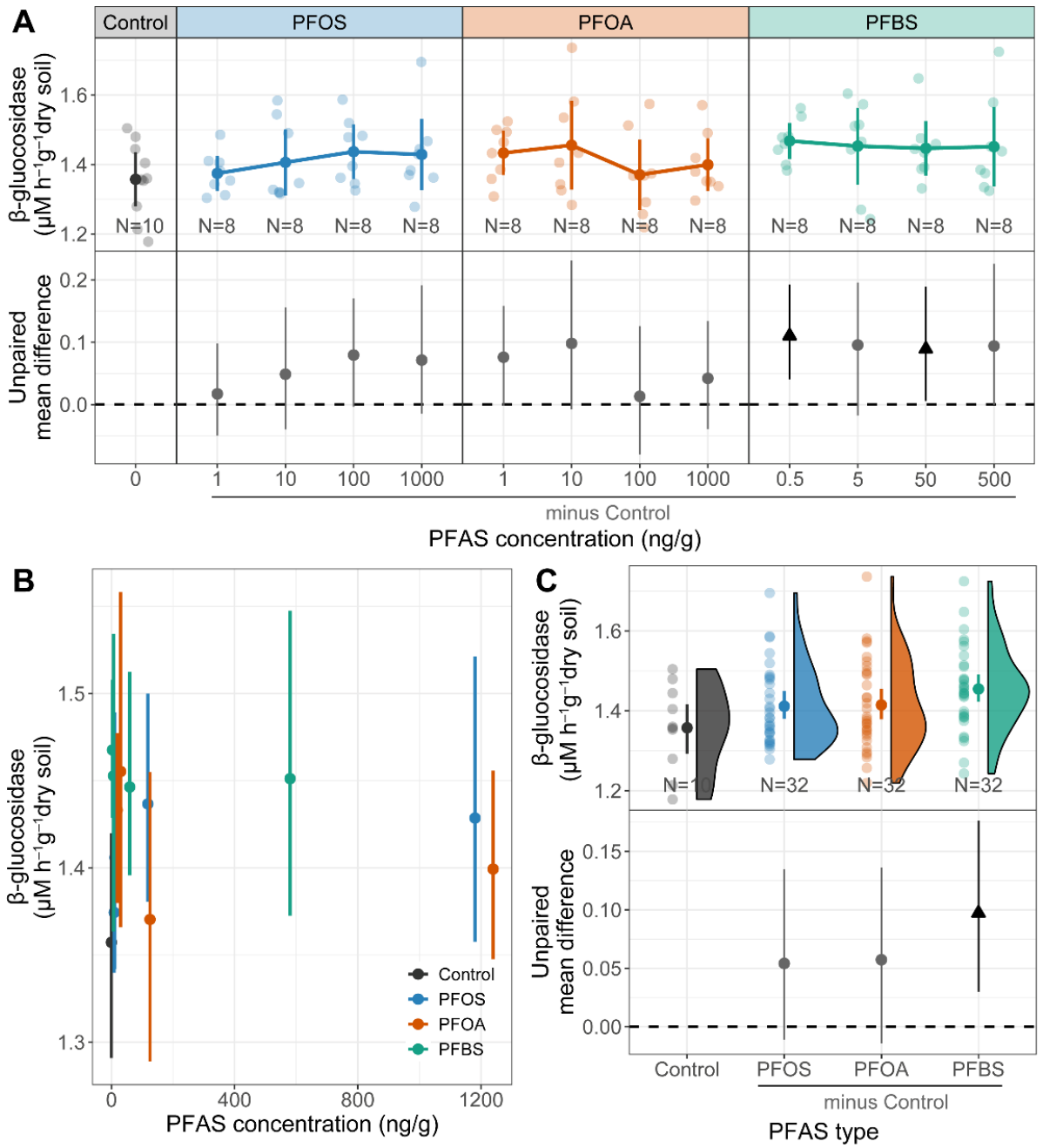

Figure S11. Effects of per- and polyfluoroalkyl substances (PFASs) on β-glucosidase activities. (A) Visualization of the effect of each PFAS on β-glucosidase activities over the range of treatment concentrations (first row). Raw data are presented as both scatter points and the corresponding mean and 95% confidence intervals (CIs) (N = 8 for each treatment, and N = 10 for blank control). (B) Summary of effects of actual PFAS concentrations on β-glucosidase activities combining treatment types. (C) Summary of PFAS type effects on β-glucosidase activities combining treatment concentrations (first row). Data in the first row of (C) are presented in raincloud plots supplemented with the corresponding mean and 95% CIs. In the second row, estimation plots present the unpaired mean difference between each

treatment and the shared control. Circles in grey represent neutral effects (95% CIs overlapping the dashed zone line), and triangles (arrow head up) in black represent positive effects (no overlapping of 95% CIs with the dashed zero line). PFOS, perfluorooctanesulfonic acid; PFOA, perfluorooctanoic acid; PFBS, perfluorobutanesulfonic acid. The outcome of ANOVA followed by Dunnett's test is presented in Table S3.

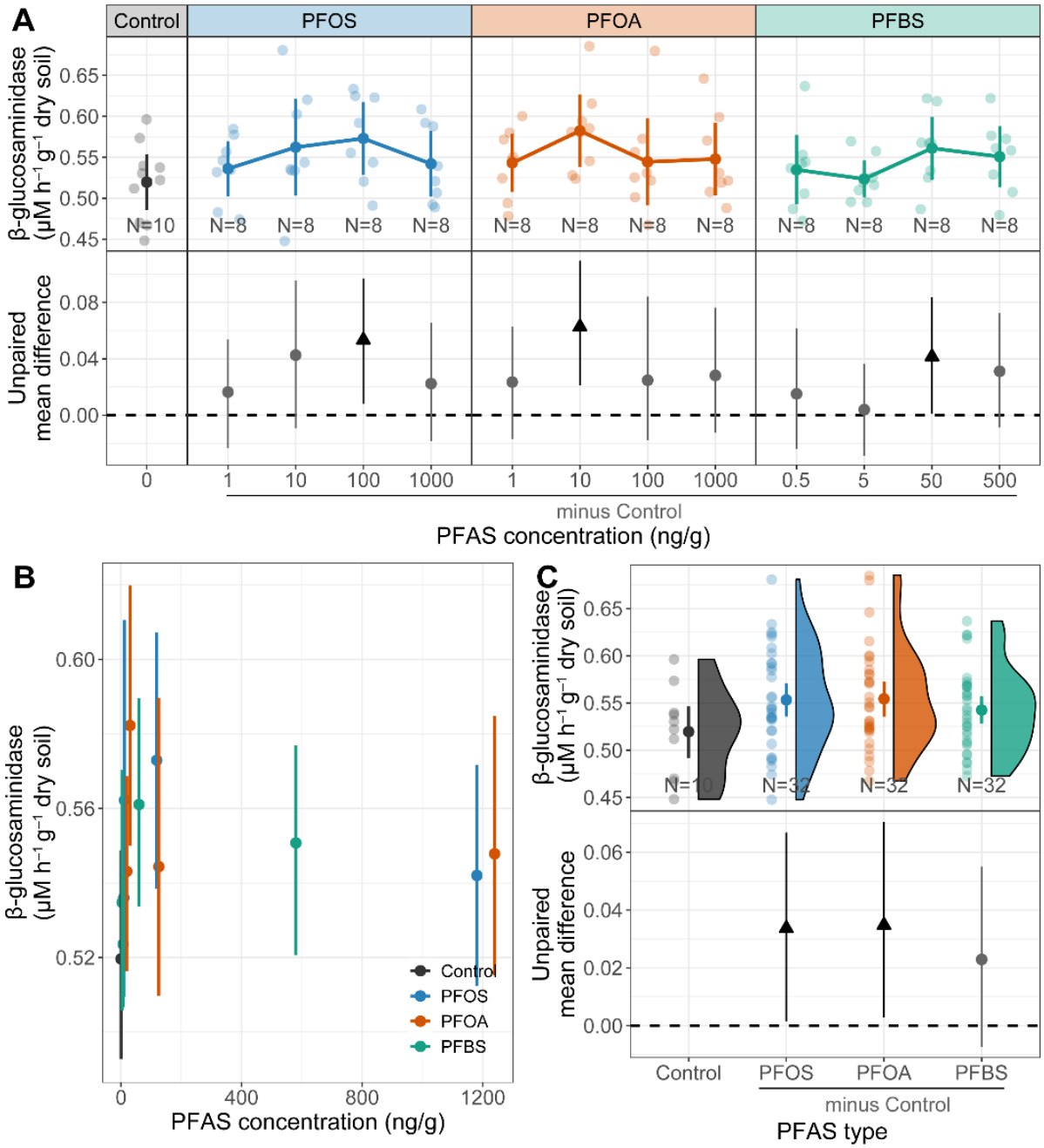

Figure S12. Effects of per- and polyfluoroalkyl substances (PFASs) on β-1,4-N-acetyl-glucosaminidase activities. (A) Visualization of the effect of each PFAS on β-1,4-N-acetyl-glucosaminidase activities over the range of treatment concentrations (first row). Raw data are presented as both scatter points and the corresponding mean and 95% confidence intervals (CIs) (N = 8 for each treatment, and N = 10 for blank control). (B) Summary of effects of actual PFAS concentrations on β-1,4-N-acetyl-glucosaminidase activities combining treatment types. (C) Summary of PFAS type effects on β-1,4-N-acetyl-glucosaminidase activities combining treatment concentrations (first row). Data in the first row of (C) are presented in raincloud plots supplemented with the corresponding mean and 95% CIs. In

the second row of each panel, estimation plots present the unpaired mean difference between each treatment and the shared control. Circles in grey represent neutral effects (95% CIs overlapping the dashed zone line), and triangles (arrow head up) in black represent positive effects (no overlapping of 95% CIs with the dashed zero line). PFOS, perfluorooctanesulfonic acid; PFOA, perfluorooctanoic acid; PFBS, perfluorobutanesulfonic acid. The outcome of ANOVA followed by Dunnett's test is presented in Table S3.

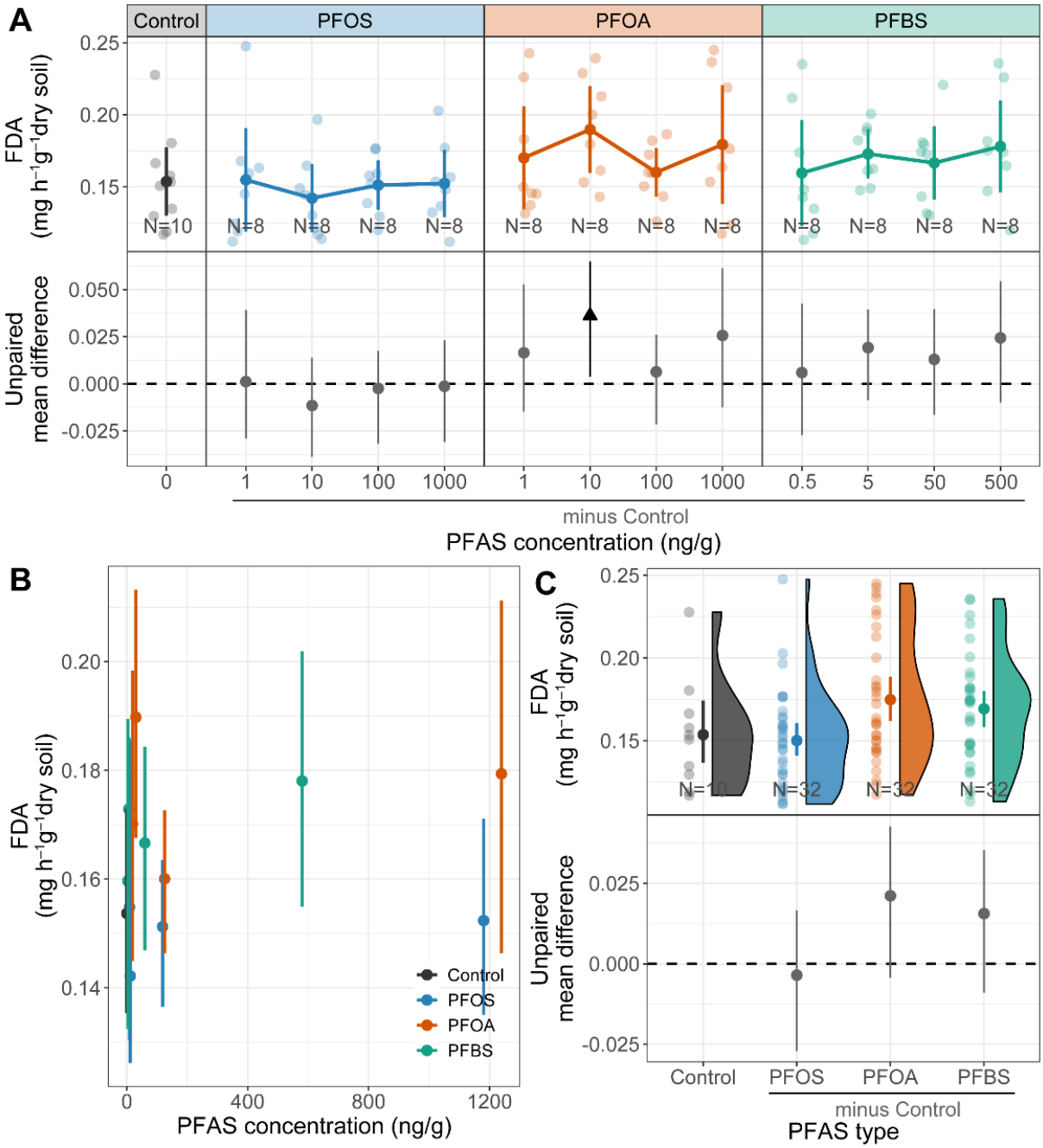

Figure S13. Effects of per- and polyfluoroalkyl substances (PFASs) on FDA activities. (A) Visualization of the effect of each PFAS on FDA activities over the range of treatment concentrations (first row). Raw data are presented as both scatter points and the corresponding mean and 95% confidence intervals (CIs) (N = 8 for each treatment, and N = 10 for blank control). (B) Summary of effects of actual PFAS concentrations on FDA activities combining treatment types. (C) Summary of PFAS type effects on FDA activities combining treatment concentrations (first row). Data in the first row of (C) are presented in raincloud plots supplemented with the corresponding mean and 95% CIs. In the second row, estimation plots present the unpaired mean difference between each treatment and the shared control. Circles in grey

represent neutral effects (95% CIs overlapping the dashed zone line), and triangles (arrow head up) in black represent positive effects (no overlapping of 95% CIs with the dashed zero line). PFOS, perfluorooctanesulfonic acid; PFOA, perfluorooctanoic acid; PFBS, perfluorobutanesulfonic acid. The outcome of ANOVA followed by Dunnett's test is presented in Table S3.

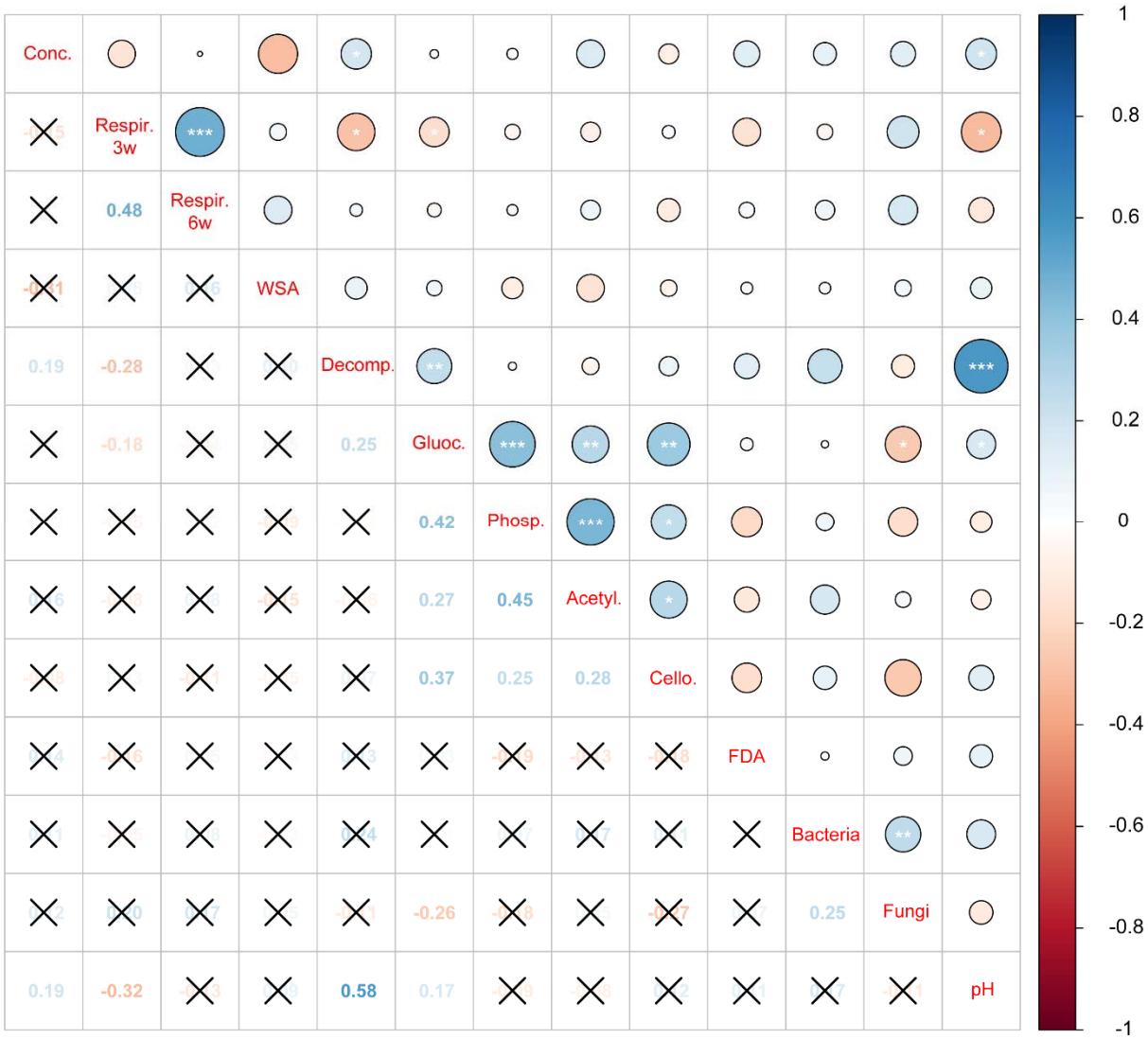

Figure S14. Spearman correlation among actual concentrations of PFAS and proxies for soil health and function. The significant levels of 0.05, 0.01, and 0.001 are presented as *, **, ***, respectively. Conc., PFAS concentration; Respir.3w, soil respiration at the 3rd week; Respir.6w, soil respiration at the 6th week; WSA, water-stable aggregates; Decomp., litter decomposition; Gluoc, β-glucosidase activity; Phosp., phosphate activity; Acetyl., β-1,4-N-acetyl-glucosaminidase activity; Cello, β-D-1,4-cellobiosidase activity; FDA, fluorescein diacetate hydrolase activity; Bacteria, soil bacterial abundance; Fungi, soil fungal abundance.

References

Jackson CR, Tyler HL, Millar JJ (2013) Determination of microbial extracellular enzyme activity in waters, soils, and sediments using high throughput microplate assays. J Vis Exp 50399. https://doi.org/10.3791/50399

Kemper WD, Rosenau RC (1986) Aggregate Stability and Size Dlstributlon. Methods soil Anal Part 1 Phys Mineral Methods

Kurz-Besson C, Coûteaux MM, Thiéry JM, et al (2005) A comparison of litterbag and direct observation methods of Scots pine needle decomposition measurement. Soil Biol Biochem 37:2315–2318. https://doi.org/10.1016/J.SOILBIO.2005.03.022

Lehmann A, Leifheit EF, Feng L, et al (2020) Microplastic fiber and drought effects on plants and soil are only slightly modified by arbuscular mycorrhizal fungi. Soil Ecol Lett. https://doi.org/10.1007/s42832-020-0060-4

Liang Y, Lehmann A, Ballhausen M-B, et al (2019) Increasing Temperature and Microplastic Fibers Jointly Influence Soil Aggregation by Saprobic Fungi. Front Microbiol 10:1–10. https://doi.org/10.3389/fmicb.2019.02018

Metzger M, Ley P, Sturm M, Meermann B (2019) Screening method for extractable organically bound fluorine (EOF) in river water samples by means of high-resolution–continuum source graphite furnace molecular absorption spectrometry (HR-CS GF MAS). Anal Bioanal Chem 411:4647–4660. https://doi.org/10.1007/s00216-019-01698-1

Milinovic J, Lacorte S, Vidal M, Rigol A (2015) Sorption behaviour of perfluoroalkyl substances in soils. Sci Total Environ 511:63–71. https://doi.org/10.1016/j.scitotenv.2014.12.017

Xie Y (2020) A meta-analysis of critique of litterbag method used in examining decomposition of leaf litters. J Soils Sediments 20:1881–1886. https://doi.org/10.1007/s11368-020-02572-9